

Chemically Induced Dynamic Nuclear Polarization

X. On Effects of Nuclear Relaxation and the Magnetic Field Dependence¹

M. LEHNIG and H. FISCHER

Physikalisch-Chemisches Institut der Universität Zürich, Schweiz

(Z. Naturforsch. 27 a, 1300—1307 [1972]; received 24 June 1972)

The magnetic field dependence of CIDNP is presented for two reaction products of independently generated alkyl radicals. It is shown that nuclear spin relaxation of the products influences the intensity distributions within multiplets, and how this relaxation can be included in the calculation of CIDNP effects from the radical pair theory. Analysis of the experimental results supports the recent view that CIDNP is created in pairs of radicals which undergo many diffusive displacements before reencounter.

1. Introduction

Chemically induced dynamic nuclear polarization (CIDNP) is currently attributed to nuclear spin dependent singlet triplet intersystem crossing in correlated radical pairs and the exclusive formation of pair products from the singlet manifold². The correlated pairs are produced by either simultaneous formation of two radicals or non-reactive radical-radical collisions. Models for calculations of the rates of product formation in the different nuclear spin states have been developed. They have been shown to yield fair agreement between observed and predicted structures of CIDNP-patterns.

It has long been realized that absolute CIDNP-enhancements are strongly influenced by the nuclear relaxation of the products². Moreover, recently, evidence for relaxation effects changing relative multiplet line intensities has been presented³. Therefore, any quantitative calculation requires the inclusion of nuclear relaxation and this aspect has so far found little attention. Further, it is known that CIDNP effects depend on the magnetic field strength during the reaction⁴. The few examples have been discussed mainly qualitatively and with neglect of relaxation effects.

This paper extends our previous analysis⁵ of CIDNP effects during reactions of independently produced $\cdot\text{CHCl}_2$, $\cdot\text{CHClCOOH}$ and $\cdot\text{CH}_2\text{COCH}_3$ radicals in solution. The product relaxation rates are determined and included in calculations of absolute enhancements during steady state conditions and of the magnetic field dependences of the CIDNP effects.

Reprint requests to Prof. Dr. H. FISCHER, Physikalisch-Chemisches Institut der Universität Zürich, CH-8001 Zürich, Schweiz, Rämistrasse 76.

2. Theoretical Considerations

The calculation of CIDNP effects requires the determination of the populations n_K of the product spin states $|K\rangle$ since the intensity of the NMR signal is

$$I(\nu) = O \cdot \sum_{L > K}^Z \sum_K^Z D_{KL}(\nu) \{n_K - n_L\}. \quad (1)$$

O is a proportionality constant, the transition probabilities $D_{KL}(\nu)$ are obtained from the chemical shifts and coupling constants J of the product, and Z is the total number of spin states. These are populated with nuclear spin dependent probabilities p_K from the radical pairs and are connected by relaxation transitions (rate constants W_{KM}), thus²

$$\frac{dn_K}{dt} = r p_K - \sum_M^Z W_{KM} \{n_K - n_M\} - (n_K^0 - n_M^0) \quad (2)$$

where r is the rate of pair formation,

$$n_K^0 - n_M^0 \cong \frac{n}{Z} \cdot \frac{\Delta E}{kT}$$

is the population difference at thermal equilibrium and $n = (\sum p_K) \int r dt'$. CIDNP effects are conveniently described by enhancement factors

$$V = (I - I^0)/I^0 \quad (3)$$

which are obtained from the intensity I at time t and the intensity I^0 observed after rapid quenching of the reaction at time t and thermal equilibration.

Under our experimental conditions⁵ we have $n_K^0 - n_M^0 \ll n_K - n_M$, thus $V \cong I/I^0$. Further we have $r \cong \text{const}$ (Section 2).

For the simplest case of a 2-level system and these conditions we obtain from (2)

$$\frac{d(n_1 - n_2)}{dt} = r(p_1 - p_2) - \frac{n_1 - n_2}{T_1} \quad (4)$$



Dieses Werk wurde im Jahr 2013 vom Verlag Zeitschrift für Naturforschung in Zusammenarbeit mit der Max-Planck-Gesellschaft zur Förderung der Wissenschaften e.V. digitalisiert und unter folgender Lizenz veröffentlicht: Creative Commons Namensnennung-Keine Bearbeitung 3.0 Deutschland Lizenz.

Zum 01.01.2015 ist eine Anpassung der Lizenzbedingungen (Entfall der Creative Commons Lizenzbedingung „Keine Bearbeitung“) beabsichtigt, um eine Nachnutzung auch im Rahmen zukünftiger wissenschaftlicher Nutzungsformen zu ermöglichen.

This work has been digitalized and published in 2013 by Verlag Zeitschrift für Naturforschung in cooperation with the Max Planck Society for the Advancement of Science under a Creative Commons Attribution-NoDerivs 3.0 Germany License.

On 01.01.2015 it is planned to change the License Conditions (the removal of the Creative Commons License condition "no derivative works"). This is to allow reuse in the area of future scientific usage.

where $T_1 = (2W_{12})^{-1}$. Integration leads to

$$V = \frac{p_1 - p_2}{p_1 + p_2} \cdot \frac{2kT}{\Delta E} \cdot \frac{T_1}{t} (1 - e^{-t/T_1}). \quad (5)$$

For $t \ll T_1$ the initial enhancement becomes

$$V_i = \frac{p_1 - p_2}{p_1 + p_2} \cdot \frac{2kT}{\Delta E} \quad (6)$$

and for $t \gg T_1$ a steady state NMR signal corresponding to

$$V_s = V_i \cdot T_1/t \quad (7)$$

is obtained.

For a multilevel system (2) leads to

$$\frac{d(n_K - n_L)}{dt} = r(p_K - p_L) - 2W_{KL}(n_K - n_L) - \sum_{M \neq L} W_{MK}(n_M - n_K) - \sum_{M \neq K} W_{ML}(n_M - n_L) \quad (8)$$

and a closed expression for V can not be obtained. However, for the initial period $t \ll (W_{KM})^{-1}$

$$V_i = \frac{\sum \sum D_{KL}(p_K - p_L)}{(\sum \sum D_{KL})(\sum p_K)} \cdot \frac{2kT}{\Delta E}. \quad (9)$$

The steady state enhancement factor V_s follows from a solution of (8) for $d(n_K - n_L)/dt = 0$. Would the last two terms of (8) reduce to a form $-\bar{w}(n_K - n_L)$ we would have again the proportionality between V_s and V_i as expressed by (7), now with $T_1 = (2W_{KL} + \bar{w})^{-1}$. Since this is not generally the case V_s is not simply proportional to V_i . This means, that except for the initial period, CIDNP patterns are influenced not only by the rates of product formation (p_K) but also by the relaxation rates W_{KL} . The latter may cause deviations from the patterns predicted from (9), i. e. under neglect of relaxation.

In the following sections we give steady state enhancement factors for $r \cong \text{const}$ in terms of the quantities^{5a}

$$\bar{V}_{s, \text{exp}} = V_{\text{exp}} \cdot t/T_1 \quad (10)$$

where T_1 is an appropriate time constant. V_i is calculated from (9) and \bar{V}_s from (1), (3) and (8). If relaxation effects are negligible, $\bar{V}_s = V_i$, therefore the differences between V_i and \bar{V}_s , and V_i and $\bar{V}_{s, \text{exp}}$ reflect the relaxation effects.

The W_{KL} and T_1 are determined from the time dependencies of CIDNP signals after interrupt of the reaction ($r = 0$). For the calculations of the p_K we use, preferentially, Adrian's high field formula⁶ for products of pairs formed by radical-radical col-

lisions:

$$p_K = 0.31 k_R (\frac{1}{2} - \frac{3}{8} k_R) + 0.105 k_R^2 \Omega_K^{1/2} \cdot \tau^{1/2} \quad (11)$$

where k_R is the probability for reaction on a singlet encounter and τ is the time between diffusive pair displacements. The matrix element Ω_K for $S-T_0$ -intersystem crossing

$$\Omega_K = \frac{1}{2} \{ (g_1 - g_2) \mu_B H_r + \sum a_{i1} m_{i1} - \sum a_{i2} m_{i2} \} \quad (12)$$

is determined from the field strength during reaction H_r and the g -factors and hyperfine coupling constants of the two radicals of the pairs. Hyperfine interactions of nuclei which do not lead to splittings in the product NMR spectra are taken into account by individual calculation of p_K for each spin state of these nuclei and summation⁶.

3. Experimental

The steady-state CIDNP proton NMR-spectra of 1,1,2-trichloropropionic acid ($\text{CHCl}_2-\text{CHClCOOH}$) and 1,1-dichloro-2-acetyethane ($\text{CHCl}_2-\text{CH}_2\text{COCH}_3$) were obtained during reactions of $\cdot\text{CHCl}_2$, $\cdot\text{CHClCOOH}$ and $\cdot\text{CH}_2\text{COCH}_3$ radicals initiated by photolysis of dibenzoylperoxide in $\text{CH}_2\text{Cl}_2/\text{CH}_2\text{ClCOOH}$ - and $\text{CH}_2\text{Cl}_2/\text{CH}_3\text{COCH}_3$ -mixtures. They have been described in Ref. ^{5a} together with the experimental details.

For the determination of the magnetic field dependencies of CIDNP the chemical systems were irradiated for $t_r = (5 \pm 0.2)$ sec in the variable field H_r of a separate magnet^{4b}. Within a few tenths of a second they were then transferred into the field $H_0 = 23.5$ kGauss of a 100 MHz-NMR-spectrometer. The transitions of the product were recorded $t_H = (7 \pm 1)$ sec after the end of irradiation. The relaxation of the polarizations at $H_0 = 23.5$ kGauss was studied by varying t_H , relaxation in the low field $H_L < 2$ Gauss of the laboratory was investigated by interrupting the transfer process for t_L seconds.

g -factors and hyperfine coupling constants of the radicals were measured by ESR. The signs of a_H in Table 1 were chosen to accommodate the phases of the

Table 1. ESR-parameters of the free radicals.

Radical	g	a [Gauss]
$\cdot\text{CHCl}_2$	2.00829	$H_\alpha: -16.79 \pm 0.05$
	± 0.00010	$^{35}\text{Cl}: \pm 3.4 \pm 0.3$ $^{37}\text{Cl}: \pm 2.9 \pm 0.3$
$\cdot\text{CHClCOOH}$	2.0070	$H_\alpha: -19.96 \pm 0.05$
	± 0.0001	$^{35}\text{Cl}: \pm 3.9 \pm 0.3$ $H(\text{COOH}): < 0.5$
$\cdot\text{CH}_2\text{COCH}_3$	2.0046	$H_\alpha: -19.69 \pm 0.05$
	± 0.0001	$H(\text{CH}_3): < 0.5$

CIDNP-patterns^{5a}. The parameters of $\cdot\text{CHClCOOH}$ and $\cdot\text{CH}_2\text{COCH}_3$ agree with previous results of other authors^{7,8}. A previous CIDNP-estimate for $\cdot\text{CHCl}_2$ ^{5a} lead to $a_H = -17.0$ Gauss and $g = 2.0080$, i. e. to values nearly identical to those now obtained. We believe that the parameter $|a_H| = 20.5$ Gauss reported by HUDSON⁹ for $\cdot\text{CHCl}_2$ is too high.

Total decomposition of dibenzoyl peroxide was lower than 5% in all experiments, thus $r = \text{const}$ holds to a very good approximation.

4. Results and Analysis

4.1. 1,1,2-Trichloropropionic Acid

The AB-system formed by the CHCl_2 and CHClCOOH protons of $\text{CHCl}_2 - \text{CHClCOOH}$ is characterized by the coupling constant $J = 6$ Hz and the difference of chemical shifts $\Delta_{AB} \cdot \nu_0 = 1.39 \cdot 10^{-6} \nu_0$, where ν_0 is the proton resonance frequency. The four transitions between the spin states $|K\rangle = \sum C_K \sigma_A^K \sigma_B^K$

$$\begin{aligned} |1\rangle &= \beta\beta \\ |2\rangle &= \sin\Theta \cdot \alpha\beta + \cos\Theta \cdot \beta\alpha \\ |3\rangle &= \cos\Theta \cdot \alpha\beta - \sin\Theta \cdot \beta\alpha \\ |4\rangle &= \alpha\alpha \end{aligned} \quad (13)$$

with $\sin 2\Theta = J \cdot (\Delta^2 \nu_0^2 + J^2)^{-1/2}$ form a characteristic AX-pattern at the observation frequency ($\nu_0 = 100$ MHz, $H_0 = 23.5$ kGauss) and are observed at the positions

$$\begin{aligned} (1) \quad \delta &= 6.19 \cdot 10^{-6} & |1\rangle \rightarrow |3\rangle, \\ (2) \quad \delta &= 6.13 \cdot 10^{-6} & |2\rangle \rightarrow |4\rangle, \\ (3) \quad \delta &= 4.81 \cdot 10^{-6} & |1\rangle \rightarrow |2\rangle, \\ (4) \quad \delta &= 4.74 \cdot 10^{-6} & |3\rangle \rightarrow |4\rangle \end{aligned}$$

(reference TMS).

Figures 1 and 2 show the magnetic field dependence of the CIDNP-intensities. A pattern observed

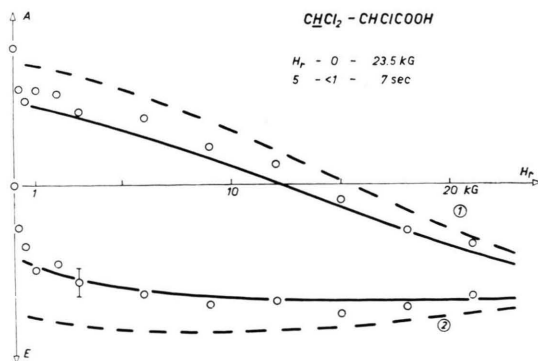


Fig. 1. Magnetic field dependence of the CHCl_2 -CIDNP-intensities of 1,1,2-trichloropropionic acid. Solid and broken lines calculated, see text; (1) in the text is identical with 1 in a circle in the figure.

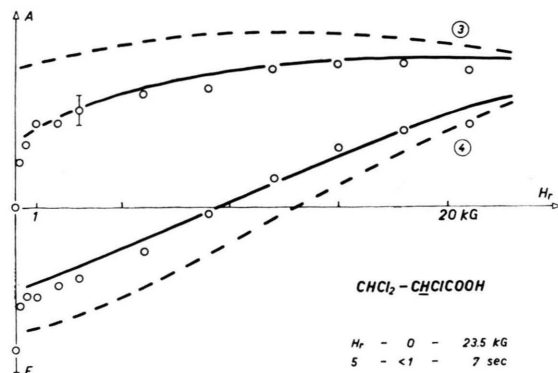


Fig. 2. Magnetic field dependence of the CHClCOOH -CIDNP-intensities of 1,1,2-trichloropropionic acid. Solid and broken lines calculated, see text.

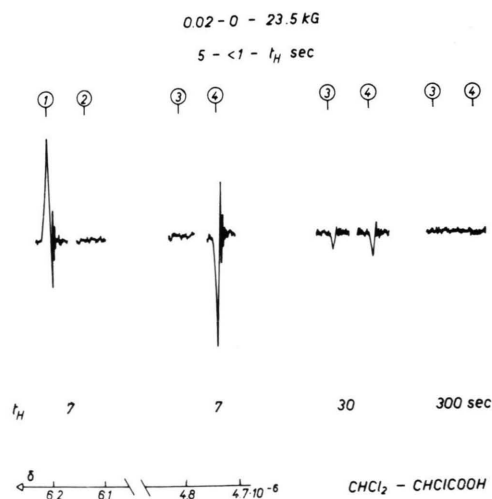


Fig. 3. Effects of relaxation in H_0 , transitions (3) and (4) of 1,1,2-trichloropropionic acid.

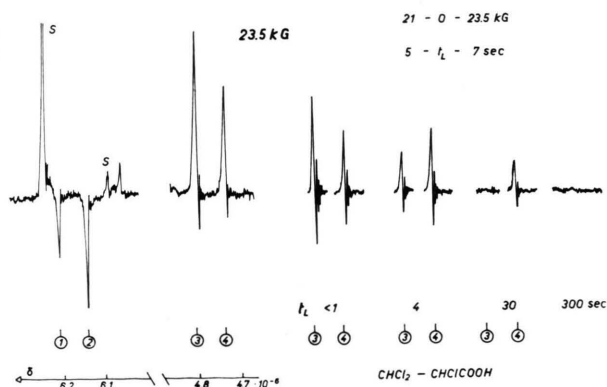


Fig. 4. Effects of relaxation in H_L , transitions (3) and (4) of 1,1,2-trichloropropionic acid.

after reaction at $H_r = 20$ Gauss is given in Fig. 3, and the steady state pattern for $H_r = H_0$ is shown in Figure 4.

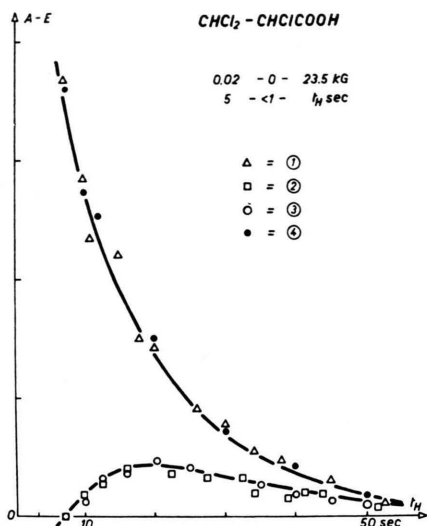
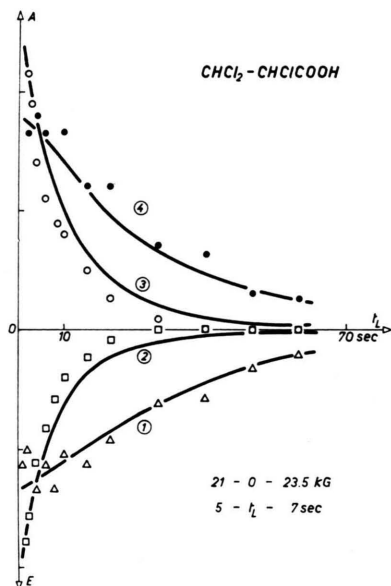
Fig. 5. Relaxation in H_0 , lines calculated, see text.Fig. 6. Relaxation in H_L , lines calculated, see text.

Figure 3 also demonstrates effects of relaxation in H_0 for lines (3) and (4). Lines (1) and (2) behave similarly, as is seen in Fig. 5 where the absolute intensities of all lines [(1) and (2) in enhanced absorption, (3) and (4) in emission] are plotted versus time t_H .

Effects of relaxation in the low laboratory field are shown in Figures 4 and 6.

For the analysis of the results we consider relaxation processes caused by randomly fluctuating ex-

ternal magnetic fields $H_{A,B}$ at the nuclei [intermolecular, $(W_{KM})_1$] and by the fluctuating intramolecular dipol-dipol-coupling between A and B [$(W_{KM})_d$]. For the intermolecular process¹⁰

$$\begin{aligned} (W_{12})_1 = (W_{21})_1 &= \frac{1}{2} \left(\frac{\sin^2 \Theta}{T_A} + \frac{\cos^2 \Theta}{T_B} + C \frac{\sin^2 \Theta}{\sqrt{T_A T_B}} \right), \\ (W_{13})_1 = (W_{31})_1 &= \frac{1}{2} \left(\frac{\cos^2 \Theta}{T_B} + \frac{\sin^2 \Theta}{T_B} - C \frac{\sin^2 \Theta}{\sqrt{T_A T_B}} \right), \\ (W_{14})_1 = (W_{41})_1 &= 0, \\ (W_{23})_1 = (W_{32})_1 &= \frac{1}{2} \left(\frac{\sin^2 2\Theta}{2 T_A} + \frac{\sin^2 2\Theta}{2 T_B} - C \frac{\sin^2 2\Theta}{\sqrt{T_A T_B}} \right), \\ (W_{24})_1 = (W_{42})_1 &= \frac{1}{2} \left(\frac{\cos^2 \Theta}{T_A} + \frac{\sin^2 \Theta}{T_B} + C \frac{\sin 2\Theta}{\sqrt{T_A T_B}} \right), \\ (W_{34})_1 = (W_{43})_1 &= \frac{1}{2} \left(\frac{\sin^2 \Theta}{T_A} + \frac{\cos^2 \Theta}{T_B} - C \frac{\sin 2\Theta}{\sqrt{T_A T_B}} \right) \end{aligned} \quad (14)$$

where for normal viscosities

$$(T_{A,B})^{-1} = \frac{2}{3} \gamma^2 |H_{A,B}|_{av}^2 \tau_D$$

are the relaxation times and τ_D is the diffusional correlation time. For the intramolecular process^{10, 11}

$$\begin{aligned} (W_{12})_d = (W_{21})_d = (W_{24})_d = (W_{42})_d &= \frac{1}{T_D} 0.1 (1 + \sin 2\Theta), \\ (W_{13})_d = (W_{31})_d = (W_{34})_d = (W_{43})_d &= \frac{1}{T_D} 0.1 (1 - \sin 2\Theta), \\ (W_{14})_d = (W_{41})_d &= 0.4 \frac{1}{T_D}, \end{aligned}$$

$$(W_{23})_d = (W_{32})_d = \frac{1}{T_D} 0.0667 \cos^2 2\Theta. \quad (15)$$

The dipolar relaxation time $T_D^{-1} = \frac{3}{2} \frac{\gamma^4 h^2}{r_{AB}^6} \tau_R$ depends on the rotational correlation time τ_R and the internuclear distance.

In a relaxation study¹⁰ of a similar AB-system (2,3-dibromothiophene, 10% in CS_2) the parameters $T_A = 92.2$ sec, $T_B = 100.2$ sec, $T_D = 87.8$ sec and $C = 0.67$ were obtained. These values allow a pre-estimate of the relative importance of inter- and intramolecular processes for our case. For the pro-

pionic acid r_{AB} is larger than for the thiophene. The viscosity of our solution (0.5 cp) is comparable to that of CS_2 . Therefore we expect $T_D \cong 87.8$ sec. On the other hand the proton density of our $CH_2Cl_2|CH_2ClCOOH$ mixture is about 10-fold larger than that of the thiophene solution. Since $|H_{A,B}|_{AV}^2$ is proportional to the proton density¹² $T_{A,B} \ll 90$ sec is anticipated. This means that $T_{A,B} \ll T_D$, so that the intramolecular process can be neglected. C seems to depend only little on r_{AB} ¹⁰, and is thus preestimated to be $C \cong 0.67$. With neglect of the dipolar process analysis of the time dependence of Fig. 5 by Eq. (2) with $r=0$ is straightforward. The symmetry immediately gives $T_A = T_B$ and $n_1 = n_4$, and the parameters of Eq. (2) reduce to T_A and the ratio $(n_2 - n_1)/(n_3 - n_1)$ at $t_H = 0$. A good fit represented by the calculated solid lines of Fig. 5 was obtained for $T_A = T_B = 19.2$ sec and $(n_2 - n_1)/(n_3 - n_1) = 0.16$ for $t_H = 0$. It will be noted that the parameter C does not enter these calculations since for the high field $H_0 \sin 2\Theta \cong 0$.

The thus determined value of $T_{A,B}$ is used as time constant T_1 in Eq. (10) to obtain the experimental steady state enhancement factors of Table 2. They differ slightly from the previously reported values^{5a} since slightly different but less defined parameters were used in the earlier study.

Table 2. Enhancement factors of 1,1,2-trichloropropionic acid.

Transition	$\bar{V}_{S, \text{exp}}$	$\bar{V}_{S, \text{calc}}$	$V_{i, \text{calc}}$
(1)	-260	-410	-375
(2)	-520	-487	-524
(3)	+740	+613	+643
(4)	+470	+535	+504

$T_A = T_B = 19.2$ sec now also enables us to calculate enhancement factors from the formulae of Section 2, (13), (14) and the radical parameters of Table 1. In these calculations the chlorine atoms of $\cdot CHCl_2$ and $\cdot CHClCOOH$ were considered to be all of mass number 35.

$$\kappa = \frac{0.31}{0.105} \cdot \frac{\frac{1}{2} - \frac{3}{8} k_R}{k_R \cdot \tau^{1/2}} \quad (16)$$

of Eq. (11) enters approximately as a linear scaling parameter into $\bar{V}_{S, \text{calc}}$ and $V_{i, \text{calc}}$. It was determined to $\kappa = 0.615 \cdot 10^6 \text{ rad}^{1/2} \text{ sec}^{-1/2}$ by a least square fit of $\bar{V}_{S, \text{calc}}$ to $\bar{V}_{S, \text{exp}}$. The results of the calculation are given in columns 3 and 4 of Table 2.

Obviously, for this example, steady state conditions and $H_0 = 23.5$ kGauss, inclusion of relaxation

does not improve the fit between experimental and calculated enhancements. The following analysis of the magnetic field dependence shows its importance more clearly.

The corresponding experiments (Figs. 1, 2, 4 and 6) involve the transfer of samples from H_r to H_L and on to H_0 , and the analysis has to start from the behaviour of the spin state populations created in H_r during the periods of transfer. There are the two limiting cases of adiabatic and non-adiabatic behaviour. For the first, the population of an eigenstate $|K\rangle$ of the product does not change with the magnetic field and follows the energy-versus-field correlation diagram. For the second, the population changes according to the projection of low field to high field eigenstates. In accord with others^{4c, 13} we believe that the adiabatic case holds for our systems, since we have compared CIDNP patterns obtained t_H seconds after reaction for t_r seconds in H_0 and no transfer with those found t_H seconds after reaction in the separate magnet for t_r seconds at $H_r \cong H_0$ and transfer and found identical spectra. For non-adiabatic transfer of populations drastic differences are expected. The finding also shows, that relaxation during transfer is negligible.

The final calculations were then performed for the conditions of adiabatic transfer, neglect of relaxation during transfer, relaxation with $T_A = T_B = 19.2$ sec in H_r and H_0 , $C = 0.67$ and the previously given parameters. The results are represented by the solid lines of Figures 1, 2 and 6. One free adjustable scaling parameter which affects the absolute intensities only was fitted to the experimental data for transitions (2) and (3). The agreement between experimental and calculated data is very satisfactory. In particular, the agreement for transitions (1) and (4) of Fig. 6 supports $C = 0.67$ since this parameter strongly influences the relaxation of these lines at $H_L \cong 0$.

The importance of full inclusion of the relaxation behaviour is demonstrated by the much poorer fit given by the broken lines of Figures 1 and 2. For the corresponding calculations relaxation was taken into account by the assumption that (8) can be approximately represented by

$$d(n_K - n_L)/dt = r(p_K - p_L) - (n_K - n_L)/T_A. \quad (17)$$

Otherwise the same parameters and scaling factor as used for the solid lines was applied. It is note-

worthy that this treatment does not yield the correct values of H_r for which the CIDNP intensities of (1) and (4) are zero.

4.2. 1,1-Dichloro-2-acetylene

At 100 MHz the $\text{CHCl}_2\text{-CH}_2\text{C}$ -group exhibits a typical AX_2 -spectrum ($J_{\text{AX}} = 6 \text{ Hz}$, $\Delta_{\text{AX}} \nu_0 = 2.76 \cdot 10^{-6} \nu_0$) with transitions at (1) $\delta = 6.32 \cdot 10^{-6}$, (2) $\delta = 6.26 \cdot 10^{-6}$, (3) $\delta = 6.20 \cdot 10^{-6}$ (CHCl_2 -group), (4) $\delta = 3.53 \cdot 10^{-6}$, (5) $\delta = 3.47 \cdot 10^{-6}$ (CH_2 -group). Steady state CIDNP-spectra for $\nu_0 = 56.4 \text{ MHz}$ and for $\nu_0 = 100 \text{ MHz}$ have been reported previously^{5a}.

The magnetic field dependence of the CIDNP-intensities are given in Figures 7 and 8. Because of experimental difficulties we were unable to measure the dependencies on t_H and t_L .

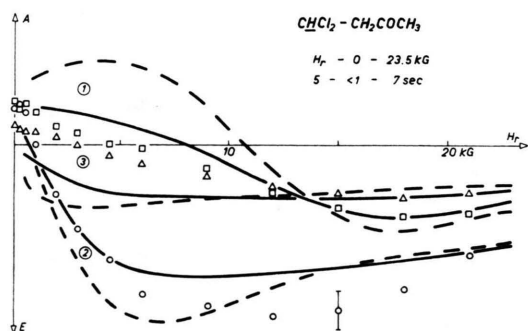


Fig. 7. Magnetic field dependence of the CHCl_2 -CIDNP-intensities of 1,1-dichloro-2-acetylene. Solid and broken lines calculated, see text.

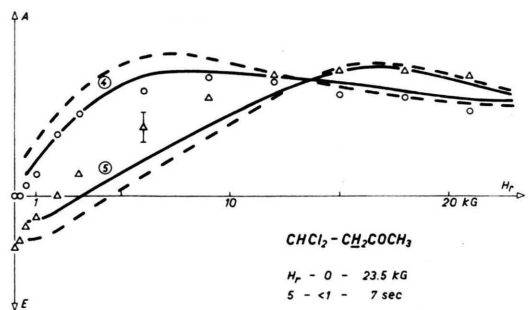


Fig. 8. Magnetic field dependence of the CH_2COCH_3 -CIDNP-intensities of 1,1-dichloro-2-acetylene. Solid and broken lines calculated, see text.

For the analysis we adopt the following relaxation model:

The CH -proton shall relax via intermolecular processes (T_A), whereas the CH_2 -protons shall relax by inter-molecular and intramolecular processes ($T_{B_1} = T_{B_2}$ and T_D). The inclusion of intramolecular di-

polar relaxation for the CH_2 -group is appropriate because the internuclear distance between the nuclei B_1 and B_2 is rather small. The same reasoning supports the further assumption that for the CH_2 -group the correlation factor $C = 1$. Calculation of the elements of the relaxation matrix for high fields (AX_2) is straight forward and will not be reproduced here¹⁴. One result of the model is the prediction that the sum of the intensities of the line group A [(1), (2), (3)] decays exponentially with the time constant $T_{1A} = T_A$, and that the sum of the intensities of group B [(4), (5)] decays with $T_{1B}^{-1} = T_B^{-1} + T_D^{-1}$ for high fields.

To determine the relaxation parameters these time constants were measured from the decay of the CIDNP-signals after reaction in H_0 . The values $T_A = 25.0 \text{ sec}$ and $T_{1B} = 12.3 \text{ sec}$ were found for 56.4 and 100 MHz. With the further assumption $T_B = T_A$, supported by the findings of Section 4.1, $T_B = 25.0 \text{ sec}$ and $T_D = 24.2 \text{ sec}$ are obtained.

These values and Eq. (10) lead to the steady state enhancement factors of column 2 in Table 3.

Table 3. Enhancement factors of 1,1-Dichloro-2-acetylene.

Transition (ν_0)	$\overline{V}_{S, \text{exp}}$	$\overline{V}_{S, \text{calc}}$	$V_{1, \text{calc}}$
(1)	- 380	- 473	- 563
(2)	- 350	- 413	- 401
(3)	- 305	- 398	- 334
(4)	+ 480	+ 456	+ 438
(5) (100 MHz)	+ 570	+ 532	+ 552
(1)	- 760	- 800	- 746
(2)	- 1180	- 920	- 988
(3)	- 800	- 796	- 713
(4)	+ 1110	+ 1035	+ 1033
(5) (56.4 MHz)	+ 965	+ 1049	+ 1052

Columns 3 and 4 of this Table show enhancement factors calculated from the formulae of Section 2 and the radical parameters of Table 1. A chlorine coupling constant of 3.9 gauss was used, the small couplings with the COOH - and COCH_3 -protons were neglected. The free scaling parameter κ (16) was obtained as $\kappa = 0.575 \cdot 10^6 \text{ rad}^{1/2} \text{ sec}^{-1/2}$ by fitting $\overline{V}_{S, \text{calc}}$ to $\overline{V}_{S, \text{exp}}$. Inspection of the enhancement factors indicates that for this example relaxation diminishes the multiplet effect type contribution² to CIDNP.

The procedure described in Section 4.1 was used in the calculation of the magnetic field dependence (Figures 7, 8). The product was treated as AB_2 -

system in the determinations of the probabilities p_K and the transition probabilities D_{KL} , whereas the relaxation matrix for an AX_2 -System was used for all fields. The latter approximation may be responsible for some deviations of calculated lines from experimental data for $H_r \lesssim 3$ kgauss. The scaling parameter was adjusted to the crossing point of transitions (4) and (5) (Figure 8). Again, proper treatment of relaxation (solid lines) gives better agreement than neglect of these processes (broken lines). However, for this example, there are significant differences between predicted and observed CIDNP effects of transitions (2) and (3) (Fig. 7) which remain to be explained.

5. Discussion

It is evident from the figures that in general relaxational effects do not grossly change the characteristics of CIDNP patterns, i. e. the net and multiplet type effects^{2,3}. They influence the intensity distribution within multiplets, however, and specifically tend to equalize the intensities of outer lines of the multiplets by intensity stealing processes. Lines predicted in emission from the p_K alone may even appear in enhanced absorption if the multiplet to which they belong has net enhanced absorption, and vice versa.

If relaxation is taken into account Adrian's high field CIDNP treatment of the probabilities p_K leads to fair qualitative and quantitative agreements of predicted and observed effects. We have not analyzed our low field data ($H_r \lesssim 1$ kgauss). Recently, GARST et al.^{4d} have treated our data of Figs. 1 and 2 in terms of a generalized Closs-Kaptein-Oosterhoff approach^{15,16}. With a free parameter τ set to $5 \cdot 10^{-10}$ sec, they have found a good fit for low fields but a rather poor fit for high fields. Relaxation was not included.

For obtaining good fits from Adrian's theory the inclusion of small hyperfine coupling constants of the radical nuclei is essential even if these nuclei do not contribute to the observed NMR patterns of the products⁶. We have previously published a magnetic field dependence of lines (3) and (4) of 1,1,2-trichloropropionic acid calculated with neglect

of the chlorine couplings¹⁷ which gave only a very poor description of the experimental data. This reference¹⁷ also shows that under neglect of the chlorine couplings a good fit is obtained from Kaptein's diffusional treatment^{4c} which in contrast to Adrian's includes a non-zero exchange interaction J between the two radicals of the pair. For the specific example $J = 2 \cdot 10^8$ rad \cdot sec $^{-1}$ was used. Our present results show that a non-zero J has not to be assumed and that this parameter simulates the effects of small nuclear coupling constants. Further, $J = 0$ supports the opinion⁶ that nuclear polarization is created in pairs which undergo many diffusive displacements before they reencounter.

The values $\alpha = 0.615 \cdot 10^6$ and $0.575 \cdot 10^6$ rad $^{1/2} \cdot$ sec $^{-1/2}$ allow estimates for the probabilities k_R of reaction during pure singlet encounters. Inserting times τ between two successive diffusive encounters of $10^{-12} \leq \tau \leq 10^{-11}$ sec into Eq. (16) we obtain $0.43 \leq k_R \leq 0.86$. These values are in accord with the definition $k_R \leq 1$ and compatible with the results of SZWARC et al.¹⁸ who obtained for the probability α of reaction during an encounter of methyl radicals $0.09 \leq \alpha \leq 0.5$.

Finally, we wish to comment on calculations of magnetic field dependencies and enhancement factors of the CIDNP effects given in Section 4 which we have performed¹⁴ using other formulations of the radical pair theory, thus as the original Closs-Kaptein-Oosterhoff^{15,16} and our kinetic¹⁹ approach. These theories contain free selectable parameters (J, τ, K) the choices of which effect the qualitative appearances of CIDNP patterns. It was possible to find parameter sets for which good fits of the experimental data are obtained even if the small coupling constants or relaxation effects were neglected and our previous work^{5a} contains some examples. Adrian's formulation⁶ does not contain such a parameter. Therefore, we believe that these parameters simply simulate effects of relaxation and small couplings which have hitherto not found attention, though the older treatments may still have their use in allowing good and quick preestimates of CIDNP spectra.

The ESR-data of Table 1 were kindly supplied by Dipl.-Phys. H. PAUL of this laboratory.

¹ Part IX: B. BLANK, P. G. MENNITT, and H. FISCHER, Spec. Lect. XXIIIrd Int. Congr. Pure Appl. Chem. **4**, 1 [1971].

² a) G. L. CLOSS, Spec. Int. XXIIIrd Int. Congr. Pure Appl.

Chem. **4**, 19 [1971]. b) H. R. WARD, Acc. Chem. Res. **5**, 18 [1972]. c) R. G. LAWLER, Acc. Chem. Res. **5**, 25 [1972]. d) H. FISCHER, Fortschr. Chem. Forsch. **24**, 1 [1971].


- ³ K. MÜLLER and G. L. CLOSS, *J. Amer. Chem. Soc.* **94**, 1002 [1972].
- ⁴ a) H. R. WARD, R. G. LAWLER, H. Y. LOKEN, and R. A. COOPER, *J. Amer. Chem. Soc.* **91**, 4928 [1969]. b) M. LEHNIG and H. FISCHER, *Z. Naturforsch.* **24 a**, 1771 [1969]. c) R. KAPTEIN, Dissertation, Leiden 1971. d) J. I. MORRIS, R. C. MORRISON, D. W. SMITH, and J. F. GARST, *J. Amer. Chem. Soc.* **94**, 2406 [1972] and work cited therein.
- ⁵ a) M. LEHNIG and H. FISCHER, *Z. Naturforsch.* **25 a**, 1963 [1970]. b) H. FISCHER and M. LEHNIG, *J. Phys. Chem.* **75**, 3410 [1971].
- ⁶ F. J. ADRIAN, *J. Chem. Phys.* **54**, 3912 [1971].
- ⁷ K. MOEBIUS, K. HOFFMANN, and M. PLATO, *Z. Naturforsch.* **23 a**, 1209 [1968].
- ⁸ M. ZELDES and R. LIVINGSTON, *J. Chem. Phys.* **45**, 1946 [1966].
- ⁹ A. HUDSON and H. A. HUSSAIN, *Mol. Phys.* **16**, 199 [1969].
- ¹⁰ R. FREEMAN, S. WITTEKOEK, and R. R. ERNST, *J. Chem. Phys.* **52**, 1529 [1970].
- ¹¹ A. ABRAGAM, *Principles of Nuclear Magnetism*, Clarendon Press, Oxford 1961.
- ¹² P. S. HUBBARD, *Phys. Rev.* **131**, 275 [1963].
- ¹³ S. H. GLARUM, private communication.
- ¹⁴ M. LEHNIG, Ph. D. Thesis, Universität Zürich 1972.
- ¹⁵ a) G. L. CLOSS, *J. Amer. Chem. Soc.* **91**, 4552 [1969]. b) G. L. CLOSS and A. D. TRIFUNAC, *J. Amer. Chem. Soc.* **92**, 2183 [1970].
- ¹⁶ R. KAPTEIN and L. J. OOSTERHOFF, *Chem. Phys. Lett.* **4**, 195, 214 [1969].
- ¹⁷ H. FISCHER, *Ind. Chim. Belg.* **36**, 1054 [1971].
- ¹⁸ a) O. DOBIS, J. M. PEARSON, and M. SZWARC, *J. Amer. Chem. Soc.* **90**, 278 [1968]. b) K. CHAKRAVORTY, J. M. PEARSON, and M. SZWARC, *J. Amer. Chem. Soc.* **90**, 283 [1968].
- ¹⁹ H. FISCHER, *Z. Naturforsch.* **25 a**, 1957 [1970].

Diffusion Slip Velocity: Theory and Experiment

H. LANG

Max-Planck-Institut für Strömungsforschung, Göttingen, Germany

and S. K. LOYALKA

 Nuclear Engineering Department, University of Missouri, Columbia, Missouri

(*Z. Naturforsch.* **27 a**, 1307—1319 [1972]; received 10 April 1972)

A theoretical and experimental study of the phenomenon of diffusion slip in a binary gas mixture is presented. To provide some physical insight, a very general variational expression given earlier by Loyalka is rederived via the use of a method developed recently. The case of Maxwellian diffuse specular reflection is considered in some detail and the inadequacies of previous theoretical results based on the early arguments of Maxwell, kinetic models and simple intermolecular force laws are discussed. Although in general, the variational results (or the equivalent results given here) together with the assumptions of Lennard Jones potential and diffusive reflection give a satisfactory agreement with the available experimental data, it is found that for isobaric (isotopic) mixtures, in the choice of the intermolecular and gas-surface interaction parameters special care should be taken in that the results are quite sensitive to small variations in the values of these parameters.

I. Introduction

Since the classical work of MAXWELL¹ it is known that velocity or temperature gradients near walls lead to the familiar surface effects of viscous and temperature slip in the range of sufficiently low pressures. These phenomena have been studied quite well both experimentally and theoretically. In the flow of gas mixtures, diffusive slip occurs due to the concentration gradient tangential to the wall. In contrast to the phenomena mentioned earlier,

little was known about this almost unstudied effect. The diffusive slip was first discussed by KRAMERS and KISTEMAKER². These authors obtained an expression for the diffusive slip by using Maxwell's momentum balance at the wall and established the existence of diffusive slip by measuring the pressure difference that results in a closed system. Since that time, this effect has been studied, both experimentally and theoretically³⁻¹⁴ by several authors. The earlier theoretical treatments, however, included only the effects of the masses and the accommodation coefficients.

A theoretical relation for the diffusion slip coefficient σ_{12} including the effects of intermolecular

Reprint requests to Dr. H. LANG, Max-Planck-Institut für Strömungsforschung, D-3400 Göttingen, Böttingerstraße 6/8.